# Effect of aspect ratio on the development of order in vibrated granular rods

Vikrant Yadav,\* Jean-Yonnel Chastaing,† and Arshad Kudrolli‡

Department of Physics, Clark University, Worcester, Massachusetts 01610, USA

(Received 5 September 2013; published 21 November 2013)

We investigate ordering of granular rods in a container subject to vibrations in a gravitational field as a function of number density of the rods. We study rods with three different length to diameter aspect ratios  $A_r = 5$ , 10, and 15. The measurements are performed in three dimensions using x-ray computer tomography to visualize the rods in the entire container. We first discuss a method to extract the position and orientation of the rods from the scans which enables us to obtain statistical measures of the degree of order in the packing. We find that the rods with  $A_r = 5$  phase separate into domains with vertical and horizontal orientation as the number density of the rods is increased, whereas, for  $A_r = 10$  and 15 the rods are predominately oriented vertically in layers. By calculating two-point spatial correlation functions, we further show that long range hexagonal order occurs within a layer when the rods are oriented along the vertical axis. Thus, our experiments find that long range order increases rapidly in granular rods with growing anisotropy.

DOI: 10.1103/PhysRevE.88.052203 PACS number(s): 45.70.Qj, 81.05.Rm

#### I. INTRODUCTION

The shape of granular materials is well known to have a significant effect on their packing properties. Spherical granular materials compact when vibrated in a container but remain disordered even when subjected to prolonged excitations [1]. By contrast, significant ordering is observed to occur with granular rods [2–4]. Development of order above a critical concentration and aspect ratio is well known in thermal rods and occurs because of maximization of configurational entropy [5]. Although these principles have been considered to predict the nature of packing of rods in the absence of gravity [6], and in vibrated rods confined to quasi-two-dimensions [7], they do not apply in general to athermal granular materials.

In the presence of gravity, experimental studies with rods in a narrow tall vertically vibrated container have found that rods with vertical orientation grow in from the boundaries [3]. It was proposed that shearing by the vertical oscillating container sidewalls was important to the observed vertical ordering. Later, rods vibrated in wide containers were shown to form domains of vertically oriented rods above a critical number density of rods when the container was vibrated vertically or horizontally [4]. These domains were observed to form everywhere within the container and not just at the boundaries. Therefore, a void filling mechanism similar to that used to understand size separation in bidisperse granular materials [8] was proposed to explain the appearance of vertically oriented rods [4]. This mechanism makes the assumption that small voids are more likely to occur than larger ones. Therefore, it is more likely that a vertical rod can fall into a void in the presence of gravity than a horizontal one. While subsequent work has further examined ordering in rods in a vertical plane [9], using simulations [10,11], and x-ray tomography [12], a full understanding of the conditions under which granular rods

order, still remains far from clear. In particular, no study exists which investigates the effect of degree of anisotropy on the development and nature of order.

In this paper, we discuss the emergence of order in vibrated rods in three dimensions (3D) enabled by a microfocus xray computer tomography (CT) instrument. This instrument allows us not only to nondestructively visualize the nature of the internal packing of rods but also to obtain quantitative information on the degree of order and defects enabled by tracking the position and orientation of all the rods in the packing. This data is then used to calculate mean orientation order parameter and the spatial pair correlation function as a function of the number of the rods in the container. We vary the aspect ratio of the rods by changing the length of the rods to investigate the impact of the degree of anisotropy on the appearance of order. As we discuss in the following, we find that only short range order is observed for the smallest aspect ratio investigated in a large container, and vertically oriented rods arranged in layers with hexagonal order are observed for higher aspect ratios.

# II. EXPERIMENTAL APPARATUS

The rods used in the experiments consist of hollow plastic cylinders and their dimensions are listed in Table I. We use hollow rods because it is easier to write algorithms to track them in 3D. The rod packings are studied within a cylindrical Plexiglas container with a diameter  $d_c=120$  mm and height  $h_c=150$  mm. The container filled with rods is mounted on a Labworks ET-139 electromagnetic shaker which vibrates sinusoidally in the vertical direction driven with a prescribed acceleration amplitude  $\Gamma$  and frequency f using an Agilent 33120A function generator. In the experiments discussed in the following  $\Gamma=3g$ , where g is the gravitational acceleration, and f=15 Hz, unless otherwise stated.

Because of the gravitational field, the rods are not uniformly distributed along the vertical axis even under the highest excitations possible in our system. Therefore, we find it convenient to use a number fraction  $n_f$  to parametrize the

<sup>\*</sup>VYadav@clarku.edu

<sup>&</sup>lt;sup>†</sup>Present address: Laboratoire de Physique, Ecole Normale Supérieure de Lyon, F-69007 Lyon. France.

<sup>‡</sup>AKudrolli@clarku.edu

TABLE I. The aspect ratio  $A_r$  and the corresponding length l and diameter d, of the hollow plastic (polypropylene) rods used in the experiments. The interrod coefficient of friction is 0.52.

$\overline{A_r}$	d (mm)	l (mm)
5	3.02	14.99
10	3.02	30.53
15	3.02	45.27

system [4] which is given by

$$n_f = \frac{n}{n_{\text{max}}},\tag{1}$$

where n is the total number of rods in the container, and  $n_{\rm max}$  is the maximum number of rods which can be packed vertically inside the container in one layer. In the container with  $d_c = 120$  mm,  $n_{\rm max} = 1450$ , corresponding to packing rods in a vertical layer with hexagonal order.

The internal imaging of the packing structure is carried out with a microfocus x-ray CT instrument manufactured by Varian Medical Systems. This instrument can image a maximum cylindrical volume with a 15 cm diameter and 15 cm height. This sets the upper limit of the sample size that we can examine. In this technique, radiograms are taken from multiple viewpoints, and a reconstruction of the 3D spatial map of the x-ray absorption by the medium is performed by the instrument. Spatial resolution of voxels with dimensions less than 100  $\mu$ m can be obtained with scans lasting 242 s using 5700 views. Even higher resolutions can be obtained with longer scans. The x-ray absorption is proportional to the amount of material in the voxel and the reconstruction algorithm yields intensity with 16-bit depth. These spatial maps can be then used to track individual rods as discussed in the next section.

Because of the time taken by the CT technique to complete the scans needed to resolve the rods inside the packing, we stop the excitation during the scan. While rods at very low concentrations (where they do not collide with each other) move rapidly under the vibration amplitudes we use, at high densities the rods do not move rapidly as they interact with multiple neighbors. Thus the rods appear to be essentially in contact and slide past each other as they rearrange. In this regime, which is the focus of our study, we find that the rods rapidly come to rest in place due to dissipation when the shaker is stopped. Therefore, the scans we analyze subsequently can be viewed as snapshots of the packing dynamics. We visually checked that turning off the excitations to obtain the scans does not affect the nature of the subsequent evolution of the packing by comparing to packings where excitations were not turned off.

### III. TRACKING THE RODS IN THREE DIMENSIONS

The various possible cross sections that a hollow tube can have are shown in Fig. 1. A typical cross section of the rod packing after the intensity map is converted to binary data, corresponding to the presence of materials (white) and void (black/blue), is shown in Figs. 2(a) and 2(b). Then we invert this image so that all rod boundaries appear dark, as shown

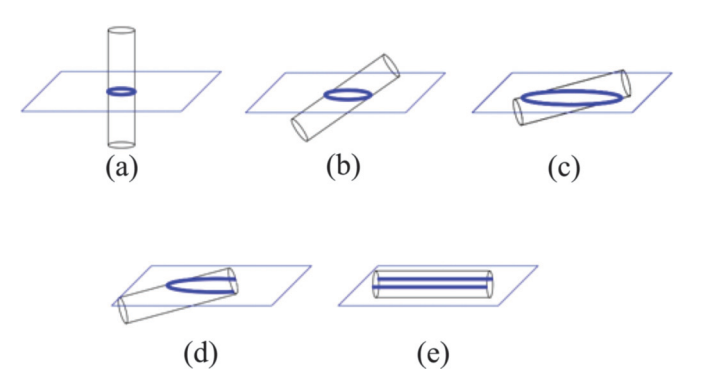


FIG. 1. (Color online) The intersection of a plane with a hollow rod can produce ellipses as in (a), (b), and (c); elliptical arcs (d); and lines as in (e).

in Fig. 2(c). A label matrix is created from this image where all connected pixels of a particular signature are denoted by the same label. As the dimensions of the rods are known, we define an upper and lower cutoff limit in terms of the pixel size that the rod cross section can have. Any size above or below these limits is discarded [see Fig. 2(d)]. To remove any false positives that are not the interior of rods we run a convexity check on the signatures. The convex area of the space exterior to rods is always larger than their true area due to the presence of kinks in their boundaries. Removing these, we are left with only the true closed signatures of the rods [see Fig. 2(e)].

We use a coordinate system with the x axis and the y axis oriented along the horizontal, and the z axis oriented along the vertical. The matrix with ellipses in a cross section can be easily tracked using a standard image processing algorithm to determine their centers in the horizontal x-y plane. We then repeat this process over all the cross-sectional images along the z axis. The cross sections belonging to the same rod in different planes are identified by proximity and are used to calculate the center of mass and orientation of each rod. Because we detect only ellipses (or closed signatures) along the one axis, we rerun the whole process for cross sections orthogonal to the x and the y axes. This enables us to track the rods which have an open signature in the x-y plane and which would be missed otherwise. Thus, we generate a list of the position and orientation of each rod in each packing for subsequent analysis.

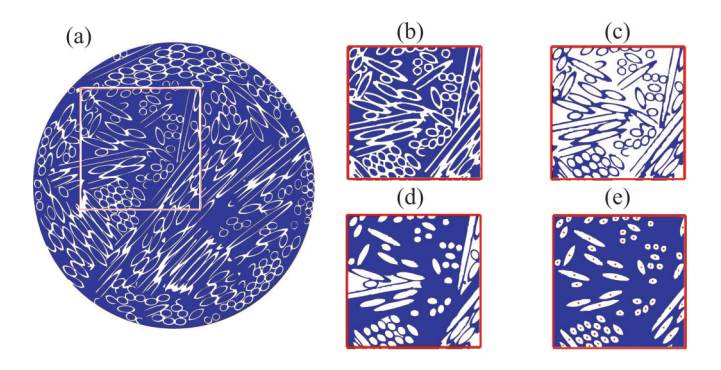


FIG. 2. (Color online) (a) A typical cross section of the packing obtained with x-ray CT scanning. The steps used to detect the rods are illustrated in (b), (c), (d), and (e) (see text). The center of a rod cross section is indicated by a dot in (e).

### IV. EVOLUTION OF ORDER

We now discuss experiments which illustrate the evolution of order when the rods are added randomly in a container and then vibrated. Figures 3(a)–3(f) show an example of the evolution when the container is vibrated over 20 min for  $n_f = 1$ . It can be noted that the rods rapidly begin to rotate toward the vertical direction everywhere within the container. Regions with hexagonal order begin to appear after only a few minutes of vibrations, and with slow healing of defects and grain boundaries occurring over time. However, we find a few defects persist even after prolonged vibrations. After inspecting the entire packing, we find that these defects are created by a few rods that get trapped at the bottom of the

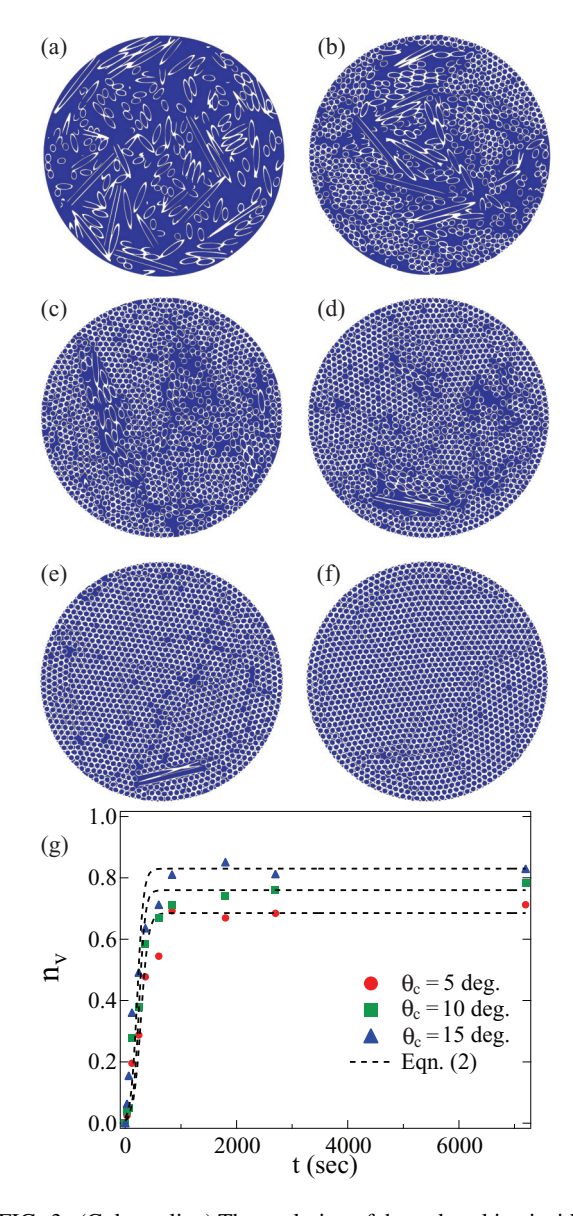


FIG. 3. (Color online) The evolution of the rod packing inside the vibrated container for  $A_r=10$  and  $n_f=1$ . The images correspond to a horizontal cross section at a height of l/2 from the bottomxbrk of the container at (a) t=0 s, (b) t=30 s, (c) t=120 s, (d) t=240 s, (e) t=840 s, and (f) t=1200 s. (g) The number fraction of rods oriented along the vertical axis. The evolution assuming the corresponding cutoff tilt angles  $\theta_c$  are also shown.

container due to the pressure of rods which have packed vertically overhead.

In order to examine the development of ordering quantitatively, we plot the ratio of the number of vertical rods  $n_v$  and the total number of rods n as a function of time in Fig. 3(g). If  $\theta$  is the angle that the rod makes with the vertical z axis, we define a cutoff tilt angle  $\theta_c$ , so that a rod is considered vertical for  $\theta < \theta_c$ . As a guide, we also plot the expected trend if the initial distribution were isotropic and if the rate of growth of vertical rods was proportional to the number of vertical rods, and independent of each other [4]:

$$\frac{\partial n_v}{\partial t} = \alpha n_v (\beta - n_v),\tag{2}$$

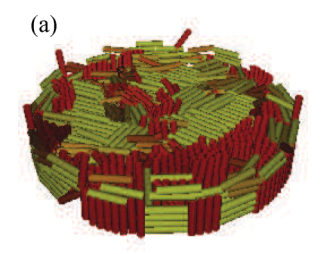
where  $\alpha$  is the rate constant, and  $\beta$  is the saturation fraction. While the final number fraction of vertical rods can be observed to change with the choice of  $\theta_c$ , the ordering is well described by Eq. (2) in each case. We find  $\alpha \approx 0.22$  independent of choice of  $\theta_c$ . And  $\beta = 0.69$ , 0.76, and 0.83 for  $\theta_c = 5{,}10$ , and 15, respectively. The rods which are not perfectly aligned (tilted at an angle greater than  $\theta_c$ ) are present in the bulk as defects, and at the top or bottom of the packing. The observed phenomena and quantitative analysis enabled by x-ray CT technique is consistent with those reported by visual inspection by Blair et al. [4]. Those experiments were performed with an order of magnitude larger number of solid brass rods and in a wider container with a container diameter to rod length ratio  $d_c/l$  which was three times larger. But, we find similar behavior while comparing across the same number fraction  $n_f$ . Thus, the smaller system size and materials used here to aid scanning does not have a qualitative influence on the observed development of order.

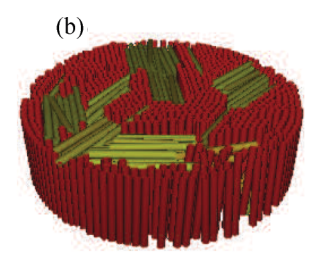
## V. NUMBER FRACTION AND ASPECT RATIO DEPENDENCE

We now examine the effect of rod aspect ratio on the observed structure at steady state as a function of the number of rods in the container. To illustrate qualitative differences which arise with aspect ratio  $A_r$ , we show snapshots of the packings observed with  $A_r = 5,10$ , and 15 for  $n_f = 1$  in Fig. 4 [13]. Here, the rods are rendered in POV-RAY using different shades which depends on the rod tilt angle  $\theta$  from the vertical. It can be noted that the rods with  $A_r = 5$  form domains of horizontal and vertical rods. The rods with larger aspect ratio  $(A_r = 10)$  have fewer horizontal rods, and are predominately oriented along the vertical axis, whereas rods with  $A_r = 15$  are seen to be all oriented vertically. Thus, we find a qualitative change in the nature of order which we characterize quantitatively next.

## A. Orientation statistics

We plot the distribution of  $\theta$  in Fig. 5 to discuss the systematic evolution of the packing as a function of  $n_f$  for each  $A_r$ . For small  $n_f = 0.1$  for each  $A_r$ , we observe that the distribution is peaked around  $90^\circ$ . This is consistent with the fact that the rods are essentially horizontal in the container due to the effect of gravity. We examined the distribution of the azimuthal orientation of the rods and found it to be isotropic because of the symmetry of the container. However, as  $n_f$  is increased the packing changes depending on  $A_r$ . In the case





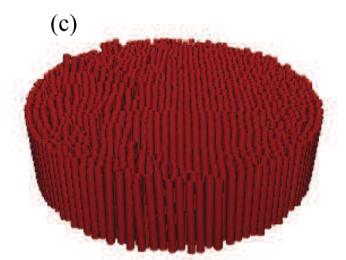


FIG. 4. (Color online) The steady state packing of rods with (a)  $A_r = 5$ , (b)  $A_r = 10$ , and (c)  $A_r = 15$  ( $n_f = 1$ ). The 3D rendering of the packing from position and orientations obtained from the x-ray CT scans. The rods with vertical and horizontal orientation are shaded red (gray) and yellow (light gray), respectively.

of  $A_r = 5$ , we observe that the distribution becomes bimodal with the peak at 90°, decreasing in amplitude, and a secondary peak developing around  $\theta = 0^\circ$ . Thus we find domains of rods which are oriented vertically and horizontally in domains

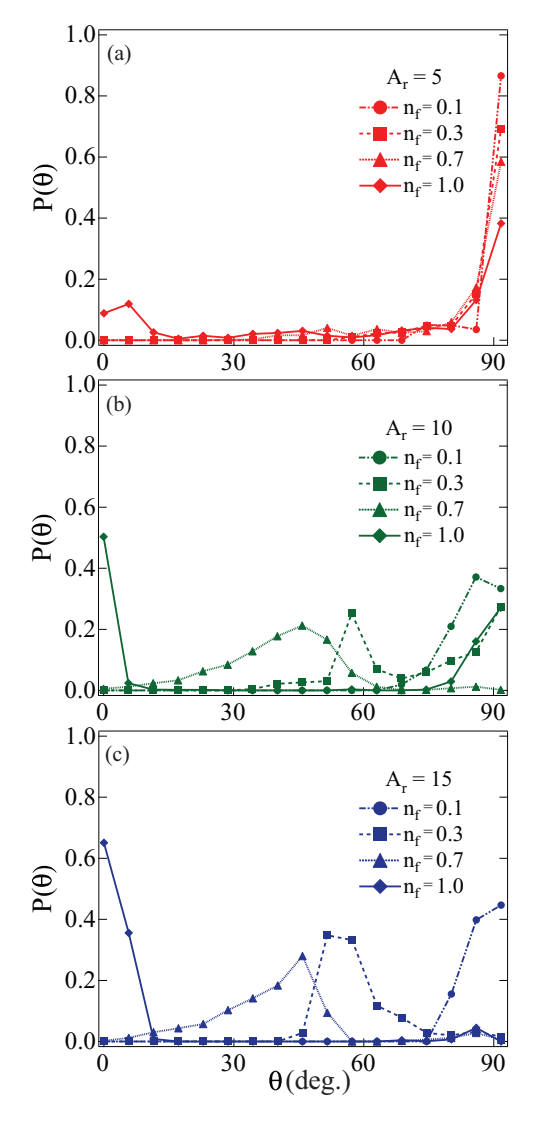


FIG. 5. (Color online) Distribution of the orientation angle of the rods with respect to the vertical for various number density and aspect ratio (a)  $A_r = 5$ , (b)  $A_r = 10$ , and (c)  $A_r = 15$ . The distribution for  $A_r = 5$  becomes bimodal with peaks near  $\theta = 0^\circ, 90^\circ$ , whereas, in the case of  $A_r = 10$  and 15, a single peak at  $\theta = 90^\circ$  develops for  $n_f = 1$ .

with few rods which are in fact at an intermediate angle. A tetratic phase has been observed in two-dimensional vibrated granular rods in the horizontal plane [14]. But the phase seen in Fig. 4(a) is somewhat different, because the orthogonal alignment of domains is in the vertical plane, but the domains appear to be randomly aligned in the horizontal plane. By contrast, a second peak is observed to develop in the case of  $A_r = 10$  at an angle which starts to decrease with  $n_f$ . This peak shows that a significant number of rods are tilted at that angle. Correlated with the appearance of this peak, we observe vortex-like motion consistent with previous observations by Blair *et al.* [4] with rods with similar aspect ratios.

As  $n_f$  approaches 1, and the tilt decreases, the vortex motion slows down and stops. This is consistent with the model for motion of rods by Volfson et~al.~[15], who showed that the convective motion arises from collision of a tilted rod with the vibrating frictional substrate. At  $n_f=1$ , we still observe a bimodal distribution of rods but the extent of horizontal defects is smaller when compared to the rod of  $A_r=5$ . The trend toward vertical orientation with  $n_f$  is even stronger in the case of  $A_r=15$ . The  $P(\theta)$  is observed to show a single peak which moves from  $\theta\approx 90^\circ$  to  $\theta\approx 0^\circ$ , and very few rods are oriented horizontally.

To have a simple measure of the global vertical order of the system, we define a parameter

$$S = \langle \cos \theta \rangle, \tag{3}$$

where,  $\langle \cdot \rangle$  represents an average over all particles in the packing, and a value of S close to 1 implies predominant alignment of rods along the vertical axis.

Evolution of S as a function of number fraction for the rods with the three different  $A_r$  is plotted in Fig. 6. We observe that as  $n_f$  is increased from 0 to 1, rods with  $A_r = 10$  and 15 go from an initially disordered state to an ordered state, whereas rods with  $A_r = 5$  do not order as significantly. We also note that the critical  $n_f$  at which ordering begins, decreases with an increase in  $A_r$ . A broad peak is seen for packing of particles with  $A_r = 5$  at low  $n_f$ . However, this does not signify actual ordering. It can be attributed to the fact that when particles with  $A_r = 5$  are vibrated at an acceleration of 3g, even at  $n_f$  close to 0.5 most of the rods are in a rare-gas-like state. When the shaker was turned off, this state quickly quenches to a static state where particles get trapped in various orientations giving an overall nonzero S.

In the case of rods with  $A_r = 10$  and 15, we observe a dip in value of S as  $n_f$  increases from 0.9 to 1. From the scans,

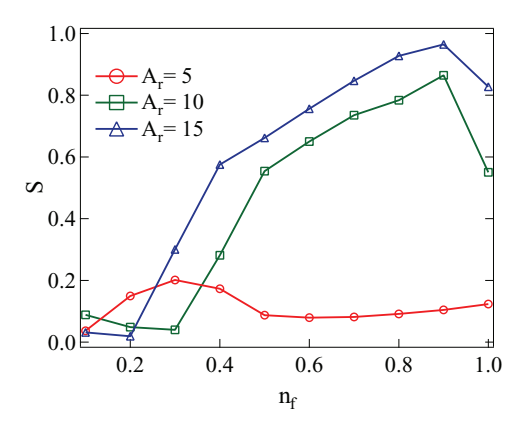


FIG. 6. (Color online) Evolution of the global vertical order parameter S as a function of  $n_f$  for rods with various  $A_r$ .

it is clear that this dip in the case of rods with  $A_r = 10$  is because of the presence of defects in the bulk of packing. In the case of rods of  $A_r = 15$ , the dip is due to the accumulation of free horizontal rods on the top of packing. As  $n_f$  tends to 1, the dynamics of the system slows down and the probability that a void can be filled by a free vertical rod near the top of the packing decreases drastically. This is because significant energy is required to rotate the rod vertically so that it can fall into a narrow void. Thus, these free rods create a dip in the value of S.

# B. Spatial order

As we can note from Fig. 4, the rods appear hexagonally ordered when oriented vertically. Therefore, we calculate the pair correlation function g(r) for different values of  $n_f$  to analyze the spatial ordering of rods within a layer. For n rods inside a volume V, g(r) as a function of distance r is given by

$$g(r) = \frac{V}{n^2} \left\langle \sum_{i} \sum_{j \neq i} \delta(\vec{r} - \vec{r_{ij}}) \right\rangle,\tag{4}$$

where  $\vec{r_{ij}}$  corresponds to the distance between particles labeled i and j, and  $\langle \cdot \rangle$  indicates averaging over the rods in the volume V.

In Fig. 7, we plot g(r) for various values of  $n_f$  and  $A_r$ . For rods with  $A_r = 5$ , there is just one primary peak at r/d = 1 because of the hard core repulsion potential between rods, and the high density of the packing. This peak becomes prominent with an increase in  $n_f$ , but no further peaks are observed. This implies a lack of local ordering in rods with  $A_r = 5$  as measured by g(r). For rods with  $A_r = 10$ , we note that there is little to no ordering at low number fractions. At  $n_f = 0.7$ , we see the emergence of a dominant first peak and a weak secondary peak. As  $n_f$  is increased further to 1.0, the secondary features of g(r) become prominent. The existence of peaks at r = d,  $\sqrt{3}d$ , 2d,  $\sqrt{7}d$ , and 3d indicated by the vertical dashed line in Fig. 7 correspond to a hexagonal lattice. Thus, the existence of a nonzero value of S that is close to 1, and the presence of a hexagonal lattice, indicates the presence of a crystalline phase. Similar signatures are observed for particles with  $A_r = 15$ . In this case additional peaks corresponding to a

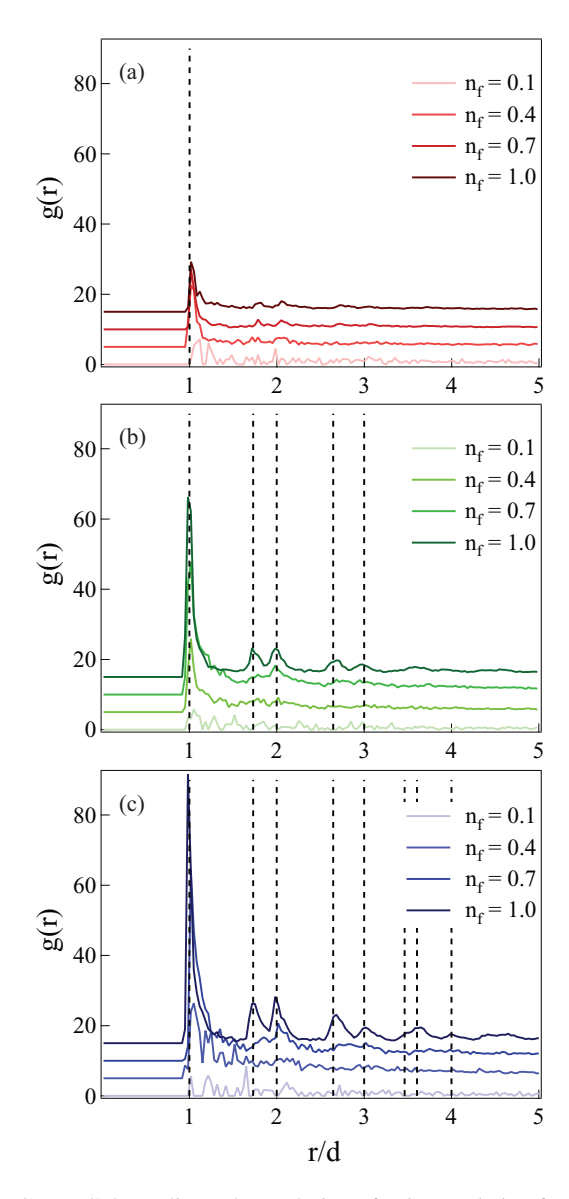


FIG. 7. (Color online) The evolution of pair correlation function g(r) as a function of distance scaled by the diameter of the rod for rods with (a)  $A_r = 5$ , (b)  $A_r = 10$ , and (c)  $A_r = 15$ . The vertical lines correspond to a hexagonal lattice.

hexagonal lattice appear in g(r) which shows that spatial order exists at even longer spatial scales.

#### VI. MULTIPLE LAYERS

We next extend our study to the case when  $n_f$  is increased above 1, and multiple layers of rods are poured into the container. In Fig. 8(a), we show the number density of the center of the rods P(z) as a function of height z obtained in steady state by vibrating rods with  $A_r = 5$  and  $n_f = 3$ . We observe sharp peaks at around l/2, 3l/2, and 5l/2 signifying the development of vertical layering with rods oriented predominately along the z axis. Further, because the amplitude of the peaks decreases with z, and the background rises, we gather that the layer at the bottom is most ordered, and the packing becomes progressively more disordered as a function of height. To further characterize the order with this

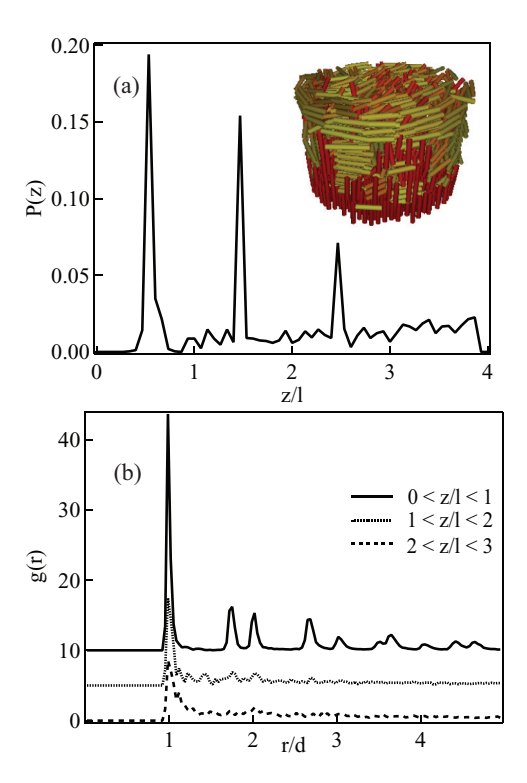


FIG. 8. (Color online) (a) Probability of finding a particle at a height z from the bottom of the container normalized with rod length l. Peaks at l/2, 3l/2, and 4l/2 indicate layering. Inset: A POV-RAY rendering of the packing observed with  $n_f=3$ . The different shades correspond to different  $\theta$  orientations as in Fig. 4. (b) g(r) within the layer shows the decreasing hexagonal order with height.

layer, we plot g(r) corresponding to each layer in Fig. 8(b). The layer at the bottom is clearly most ordered with peaks corresponding to the hexagonal lattice. However, disorder grows with height.

The greater order in the lower layers occurs because of at least two factors. First, the voids that are created in the first layer due to vibrations are filled more efficiently due to vertical rods falling from top layers into the bottom layer. Further, horizontally oriented rods are more likely to be blocked from falling through the gaps between the rods by other rods. This leads to an increase in the number of horizontal rods with height. Secondly, energy is input into the system due to collisions of the rods with the vibrating bottom of the container. But this energy is lost because of inelastic collisions among rods as it reaches the upper layer. Because of this decrease in

energy, the effective rods fluctuations (granular temperature) decreases with height. Thus, the frequency of creating voids decreases with height, and there is less energy available to cause a horizontal rod to rotate to a more vertical orientation. Therefore, defects that are initially present may not evolve significantly, and the packing remains in a disordered state even after being subject to prolonged vibrations.

### VII. CONCLUSION

In summary, we investigated the evolution of the ordering transition in vibrated granular rods as a function of their number fraction and aspect ratio with x-ray tomography. We discussed a method to track the rods in 3D which is then used to calculate the microstructural properties of the system. We find that the degree of ordering increases with the aspect ratio of rods. From the distribution of the vertical component of orientation vector of rods, we showed that rod packings with all aspect ratio have some ordering as their number fraction is increased. Using mean orientation data we could also show that rods with larger aspect ratio were more ordered. Pair correlation functions are used to show that rods tend to arrange themselves in a hexagonal lattice in a layer, and further that range of ordering increases with aspect ratio of the rods. We further found that the ordering extended into multiple layers as  $n_f$  was increased above 1. However, the ordering decreases from the bottom to the top layer because of decreased energy transfer to higher layers from the container bottom due to the dissipative nature of the system.

The experiments and the quantitative analysis are overall consistent with the void filling mechanism for development of vertical order. However, it is unclear why the rods with  $A_r = 5$  phase separate into horizontal and vertical rod domains, and simply do not form a more broader angle distribution centered around the vertical. The development of hexagonal order with a layer of vertically oriented rods is consistent with the fact that the maximum packing of rods lowers the center of mass of the entire packing. However, analytical results on the effect of rod aspect ratio on the degree of order are not available to further analyze the system. It is hoped that this experimental investigation will enable further development of a theory of ordering in athermal granular rods in a gravitational field.

#### ACKNOWLEDGMENT

This work was supported by the National Science Foundation Grants No. CBET-0853943 and No. DMR-0959066.

<sup>[1]</sup> J. B. Knight, C. G. Fandrich, C. N. Lau, H. M. Jaeger, and S. R. Nagel, Phys. Rev. E 51, 3957 (1995).

<sup>[2]</sup> P. Ribiere, P. Richard, D. Bideau, and R. Delannay, Eur. Phys. J. E 16, 415 (2005).

<sup>[3]</sup> F. X. Villarruel, B. E. Lauderdale, D. M. Mueth, and H. M. Jaeger, Phys. Rev. E **61**, 6914 (2000).

<sup>[4]</sup> D. L. Blair, T. Neicu, and A. Kudrolli, Phys. Rev. E 67, 031303 (2003).

<sup>[5]</sup> L. Onsager, Ann. N.Y. Acad. Sci. 51, 627 (1949).

<sup>[6]</sup> C. C. Mounfield and S. F. Edwards, Physica A 210, 290 (1994)

<sup>[7]</sup> J. Galanis, D. Harries, D. L. Sackett, W. Losert, and R. Nossal, Phys. Rev. Lett. 96, 028002 (2006).

<sup>[8]</sup> A. Kudrolli, Rep. Prog. Phys. 67, 209 (2004).

<sup>[9]</sup> G. Lumay and N. Vandewalle, Phys. Rev. E **74**, 021301 (2006)

- [10] L. Pournin, M. Weber, M. Tsukahara, J. A. Ferrez, M. Ramaioli, and Th. M. Liebling, Granular Matter 7, 119 (2005).
- [11] M. Ramaioli, L. Pournin, and Th. M. Liebling, Phys. Rev. E **76**, 021304 (2007).
- [12] Y. Fu, Y. Xi, Y. Cao, and Y. Wang, Phys. Rev. E **85**, 051311 (2012).
- [13] See Supplemental Material at http://link.aps.org/supplemental/ 10.1103/PhysRevE.88.052203 for movies of the scan of the packings.
- [14] V. Narayan, N. Menon, and S. Ramaswamy, J. Stat. Mech. (2006) P01005.
- [15] D. Volfson, A. Kudrolli, and L. S. Tsimring, Phys. Rev. E 70, 051312 (2004).